THE JOURNAL OF PHYSICAL CHEMISTRY B

ARTICLE

pubs.acs.org/JPCB

Characterization of Supported Lipid Bilayer Disruption By Chrysophsin-3 Using QCM-D

Kathleen F. Wang,[†] Ramanathan Nagarajan,[‡] Charlene M. Mello,[‡] and Terri A. Camesano*[,†]

[†]Department of Chemical Engineering, Worcester Polytechnic Institute, Worcester, Massachusetts 01609, United States

[‡]Natick Soldier Research, Development and Engineering Center, Molecular Sciences and Engineering Team, Natick, Massachusetts 01760, United States

ABSTRACT: Antimicrobial peptides (AMPs) are naturally occurring polymers that can kill bacteria by destabilizing their membranes. A quartz crystal microbalance with dissipation monitoring (QCM-D) was used to better understand the action of the AMP chrysophsin-3 on supported lipid bilayers (SLB) of phosphatidylcholine. Interaction of the SLB with chrysophsin-3 at 0.05 μM demonstrated changes in frequency (Δf) and energy dissipation (ΔD) that were near zero, indicating little change in the membrane. At higher concentrations of chyrsophsin-3 (0.25−4 μM), decreases in Δf of up to 7 Hz were measured. These negative frequency changes suggest that mass was being added to the SLB, possibly due to peptide insertion into the membrane. At a chrysophsin-3 concentration of 10 μM, there was a net mass loss, which was attributed to pore formation in the membrane. QCM-D can be used to describe a mechanistic relationship between AMP concentration and interaction with a model cell membrane.

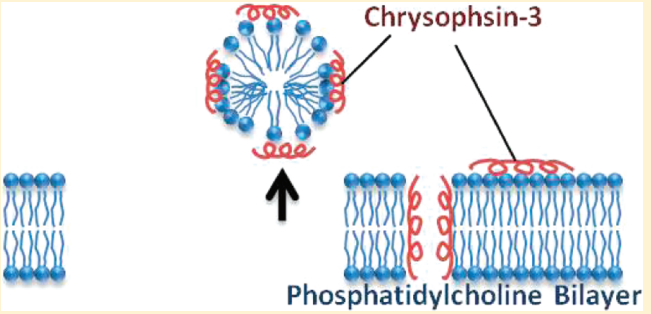

INTRODUCTION

Antimicrobial peptides (AMPs) serve as a natural defense for living organisms against pathogenic bacteria. They can be derived from various organisms, including frogs, moths, and pigs, as well as synthesized.[1,2] AMPs exhibit broad-spectrum activity against bacteria and are less prone to the development of pathogen resistance than antibiotics. Increasing concerns over antibiotic-resistant pathogens and public health issues have led to interest in using AMPs therapeutically and in self-decontaminating surfaces.[3,4] For example, omiganan, a synthetic cationic peptide, has been shown to inhibit the growth of pathogens that cause catheter-associated infections, such as Gram-positive *Staphylococcus aureus* and Gram-negative *Pseudomonas aeruginosa* (*P. aeruginosa*).[5]

The ability of AMPs to avoid pathogen resistance is largely due to the mechanism by which they kill bacteria. AMPs attach to bacterial cell membranes and, at a critical concentration, cause the cells to lyse by disrupting the membrane.[6] However, the mechanism of cell lysis is not well understood. The attachment of AMPs to cells, such as cecropin P1 to *Escherichia coli*, has been studied, but questions remain on the exact nature of the cecropin P1−*E. coli* interaction.[7,8] Detailed knowledge of the mechanism behind AMP action is essential for developing applications that make use of AMPs, such as biosensors or AMP-coated materials.

Two main theories have been proposed to explain how AMPs destabilize bacterial cell membranes. In each case, the AMPs first attach to components of bacterial surfaces through electrostatic interactions.[9] The carpet model supposes that AMPs align themselves parallel to the membrane surface, which is facilitated by their amphipathicity. AMPs surround the lipids, and micelles break off from the lipid membrane. In the barrel-stave model, the AMPs insert themselves into the bacterial cell membrane perpendicularly and form a pore.[10,11] The pores enable large molecules to enter or exit the cell and disrupt ion gradients, causing the cell to die. The disruption of the lipid membrane may also allow AMPs to enter the cell and destroy intracellular components.[8] The mechanism is thought to differ among AMPs and is related to the structure and charge of the peptide, as well as the lipid composition of the cell membrane.[12,13] For some cases, both micelle formation and pore insertion may occur, depending on the peptide-to-lipid concentration ratio.[14]

The peptide investigated in this study is chrysophsin-3, a histidine-rich AMP that is found in red sea bream gills. The red sea bream, *Chrysophrys major*, secretes AMPs from exposed areas, such as gills, to defend itself against bacterial infection.[15] Chrysophsin-3 consists of 20 amino acids in an α-helical structure, which is highly cationic and amphipathic (Figure 1). It exhibits antimicrobial activity against Gram-positive and Gram-negative pathogenic bacteria and exhibits hemolytic activity at approximately 1 μM.[16] AMPs have been shown to be effective against *P. aeruginosa* in vivo using rat models, suggesting that AMPs may still be used clinically, despite their hemolytic properties.[17] Peptide mimics may also play a role in therapeutic treatments, as chrysophsin-3 can be made less harmful to eukaryotic cells by removing the characteristic C-terminal RRRH amino acid sequence.[18]

In this study, a supported phosphatidylcholine (PC) bilayer was used as a model zwitterionic membrane to observe the interaction

Received: October 7, 2011
Revised: November 13, 2011
Published: November 15, 2011

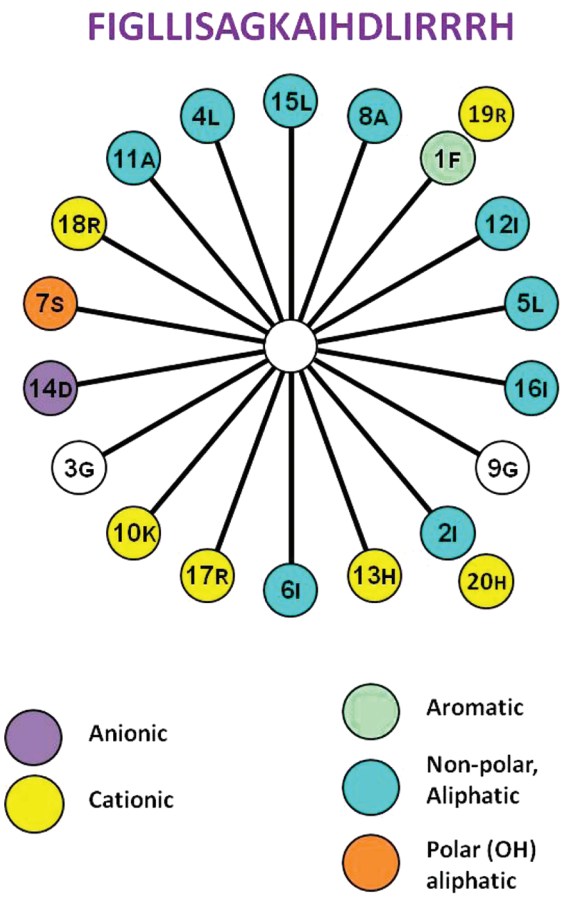

Figure 1. Helical wheel diagram of chrysophsin-3. The diagram represents the peptide viewed along the axis of the helix, in which the peptide backbone is shown by the inner circle and the spokes represent amino acids. The amino acids are numbered according to their sequence. The helical wheel diagram reveals the concentration of amino acids with positively charged side chains on one side of the helix and the clustering of nonpolar, aliphatic side chains.

between chrysophsin-3 and a cell. Phospholipid vesicles have been studied extensively for their ability to self-assemble into planar bilayers on solid surfaces.[19,20]

Quartz crystal microbalance with dissipation (QCM-D) monitoring was used to investigate the mechanism behind the peptide–lipid system of chrysophsin-3 and PC. QCM-D has become a valuable tool for monitoring real-time mass changes of various biological systems, including fatty acid attachment to supported lipid bilayers and cell adsorption to fibronectin.[21,22] Frequency and dissipation measurements at various overtones can be used to determine the nature of mass attachment to a quartz sensor crystal.

Overtone analysis was used by Mechler et al. to infer details about the fundamental mechanisms behind AMP action on supported bilayers. Similar changes in frequency (Δf) and dissipation (ΔD) at all overtones indicate a homogeneous change in mass and viscoelasticity of the membrane on the crystal's surface. Studies exposing lipids 1,2-dimyristoyl-*sn*-glycero-3-phosphocholine (DMPC) and 1,2-dimyristoyl-*sn*-glycero-3-phospho-*rac*-(1-glycerol) (DMPG) to 1–20 μM concentrations of peptides aurein 1.2, maculatin 1.1, and caerin 1.1 resulted in qualitative and quantitative differences in the frequencies that were specific to each system.[23]

Monitoring overtone similarity can provide significant information about the mechanism of action of AMPs on a lipid bilayer

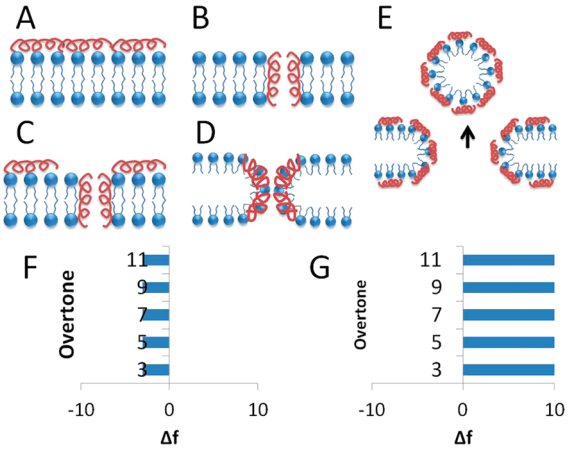

Figure 2. Possible mechanisms of peptide action on cell membranes (A–E) and corresponding estimated Δf values (F–G). (A) Monolayer of peptide adsorbed on the lipid bilayer surface. (B) Cylindrical pore formation. (C) Pore formation with adsorption. (D) Toroidal pore: lipids bend at the pore site to create a toroidal shape around peptides forming a pore. (E) Large pore formation. Negative Δf values indicate mass addition (F), which may occur in A–D. Positive Δf values indicate mass removal (G), which corresponds to the large pore formation shown in E. The baseline at $\Delta f = 0$ would indicate the presence of a bilayer on the QCM-D crystal.

surface. The barrel-stave model for peptide–membrane interactions should ultimately result in uniformly negative Δf and ΔD values at all overtones, which would represent cylindrical pore formation (Figure 2B, F). In the case of toroidal pore formation, however, more lipid would be lost at the top and bottom of the bilayer and replaced by pore-forming peptides, resulting in heterogeneous frequency changes at different overtones (Figure 2D). Initial adsorption of AMPs onto the membrane surface will theoretically result in nonhomogeneous negative changes in frequency if no other action occurs (Figure 2A). Since the changes occur primarily on the surface of the membrane, the adsorption process will not be homogeneous throughout the membrane, which would result in different response at various overtones. Combinations of membrane surface adsorption and pore formation will result in nonuniform Δf results across overtones (Figure 2C). Given that a full PC bilayer (~5 nm thick) assembled on a clean QCM-D crystal corresponds with a Δf of ~−26 Hz, we can calculate the approximate Δf due to adsorption of a monolayer of α-helical peptides (~1.2 nm thick) to be ~2–4 Hz.[20,24] Therefore, if the carpet model is operative, membrane lysis will be demonstrated through uniform positive Δf values up to 26 Hz at all overtones (Figure 2E, G).

The action of chrysophsin-3 on a PC membrane supported on a QCM-D sensor crystal was monitored in real time in this study. Changes in frequency and dissipation were monitored when chrysophsin-3, at concentrations between 0.05 and 10 μM, interacted with the PC bilayer. Values of Δf and ΔD were also monitored after rinsing the system with buffer to remove any unattached particles and to reveal the irreversible effect of peptide on the lipid bilayer. QCM-D data are used to propose a mechanism for how chrysophsin-3 interacts with cell membranes.

EXPERIMENTAL METHODS

Vesicle and Peptide Preparation. Lyophilized powder PC derived from chicken egg yolk was purchased from Sigma Aldrich

(St. Louis, MO) and Avanti Polar Lipids (Alabaster, AL). PC was dissolved in ethanol to create 100 mg/mL stock solutions that were stored at −15 °C. A buffer of 100 mM sodium chloride and 10 mM tris(hydroxymethyl)aminomethane (Sigma-Aldrich, St. Louis, MO) at pH 7.9 was prepared in ultrapure water.[25]

The PC stock solution was measured and dried with nitrogen gas to remove the ethanol. Dried lipids were placed in a vacuum desiccator overnight and suspended in buffer at 2.5 mg/mL.[26] The lipid mixture was vortexed and homogenized through five freeze−thaw and subsequent vortexing cycles.[20]

Small unilamellar vesicles (SUVs) were formed by sonicating the mixture in a glass test tube with an ultrasonic dismembrator (model 150T, Fisher Scientific, Waltham, MA) for 30 min in pulsed mode with a 30% duty cycle (3 s pulse at an amplitude of 60, followed by a 7 s pause) at 0 °C. Probe particles were removed from the solution through centrifugation (Sorvall Discovery 100SE, Kendro, Newtown, CT) at 15 000 rpm (38 500*g*) for 10 min at 4 °C. The supernatant containing the SUVs was collected and stored at 4 °C under nitrogen for up to 5 weeks.[20] Dynamic light scattering experiments (Zetasizer Nano ZS, Malvern, Worcestershire, UK) revealed the size of the vesicles to be approximately 37 nm in diameter. The stock solution was diluted to 0.1 mg/mL for each experiment.

Chrysophsin-3 (FIGLLISAGKAIHDLIRRRH) was purchased from Bachem (Torrance, CA) and stored at −15 °C. Samples were prepared at chrysophsin-3 concentrations of 0.05, 0.25, 1, 2, 4, and 10 μM in tris buffer. Solutions were brought to 23 °C before use in experiments.

Quartz Crystal Microbalance with Dissipation Monitoring (QCM-D). QCM-D measurements were performed using the Q-SENSE E4 system (Biolin Scientific, Sweden). Quartz sensor crystals were placed into the QCM-D's four chambers and exposed to solutions of buffer, lipids, or peptides. We measured overtones, or harmonics, of the resonant frequency and the energy dissipation of the sensors as mass attached to the exposed silica-coated surfaces. The normal mass and dissipation sensitivities of QCM-D measurements in liquid are ~1.8 ng/cm^2 and ~0.1×10^{-6}, respectively.

The Sauerbrey equation describes the relationship between Δf and change in mass (Δm) in a rigid film

$$\Delta f = \frac{-2f_0^2}{A\sqrt{\rho_q \mu_q}}\Delta m \quad (1)$$

where f_0 is the resonant frequency of the quartz crystal (5 MHz); A is the peizoelectrically active crystal area; ρ_q is the density of quartz (2.648 g/cm^3); and μ_q is the shear modulus of the crystal (2.947×10^{11} g/cm·s^2). Therefore, the change in frequency is inversely related to the change in mass attached to the sensor. However, in the case of a less rigid film, the Sauerbrey equation must be adjusted to reflect the effects of a viscoelastic film and the bulk solution.[27,28] Changes in dissipation are related to the rigidity of the film and can be described by

$$D = \frac{G''}{2\pi G'} \quad (2)$$

where G'' is the loss modulus and G' is the storage modulus. A softer film will result in a larger ΔD.

Table 1. Penetration Depths of Different Overtones in Water and in a Membrane

overtone number	penetration depth in water (ρ_f = 1 g·cm^{-3}, η_f = 0.01 g·cm^{-1}·s^{-1})[a]	penetration depth in membrane (ρ_f = 1 g·cm^{-3}, η_f = 1 g·cm^{-1}·s^{-1})[a]
3	146 nm	14.6 nm
5	113 nm	11.3 nm
7	95 nm	9.5 nm
9	84 nm	8.4 nm
11	76 nm	7.6 nm

[a] ρ_f and η_f are the density and viscosity of the film, respectively.

Different harmonics of a sensor crystal can be correlated with changes in various depths of a film deposited on the crystal. The penetration depth, δ, of an acoustic wave can be found

$$\delta = \left(\frac{\eta_f}{n\pi f_0 \rho_f}\right)^{1/2} \quad (3)$$

where η_f is the viscosity of the film; n is the overtone number; and ρ_f is the density of the film.[29] Penetration depths of various overtones are greater in water than in a membrane (Table 1).

QCM-D measurements can be sensitive to changes in viscosity and density of the bulk solution, which can complicate interpretation of the data. Bordes and Höök developed methods to quantify the bulk response and separate the bulk effect from the response of the adsorbed mass. The measured Δf is effectively a sum of the Δf of the adsorbed mass and Δf of the bulk solution (where the frequencies are normalized to each overtone).[30] The bulk solution effect in these experiments, which consists of the buffer, lipids, and/or AMPs, was determined to be negligible at the measured harmonics, which were the 3rd−11th harmonics of the sensor crystal's natural frequency (5 MHz). Due to the low concentrations of AMPs and lipids used, the viscosity and density of the solutions would not change enough to produce a significant effect on the measured frequencies. The measured harmonics were normalized to each overtone (f/n, where f is frequency and n is the harmonic number) by the Q-SENSE software. The fundamental frequency was not analyzed due to a higher sensitivity to changes in the bulk solution during flow.[23]

Sensor Preparation. Silica-coated sensor crystals were placed into the QCM-D flow chambers and cleaned by flowing ultrapure water, 2% sodium dodecyl sulfate solution (Sigma, St. Louis, MO), and ultrapure water through the system. The sensors and chambers were dried with nitrogen gas. A Plasma Prep II oxygen plasma cleaner (SPI Supplies, West Chester, PA) was used to etch the sensor surface before each experiment to remove the outer atomic layers of the crystal surface and make it more hydrophilic. This latter step facilitates vesicle rupture into a bilayer.

Bilayer Formation and Peptide Exposure. Buffer was flowed over QCM-D sensors at 0.15 mL/min for ~15 min until the frequency and dissipation responses were stable. The lipid SUV solution was flowed over the crystals for ~8 min to form a stable supported lipid bilayer (SLB). The crystals were rinsed with buffer to remove any unattached lipids. After establishing a baseline, peptide solution was added for 10 min, at which time the pump was stopped. QCM-D crystals were exposed to a stagnant peptide solution for 1 h, after which the peptide solution was replaced with a final buffer rinse at 0.15 mL/min until the frequency

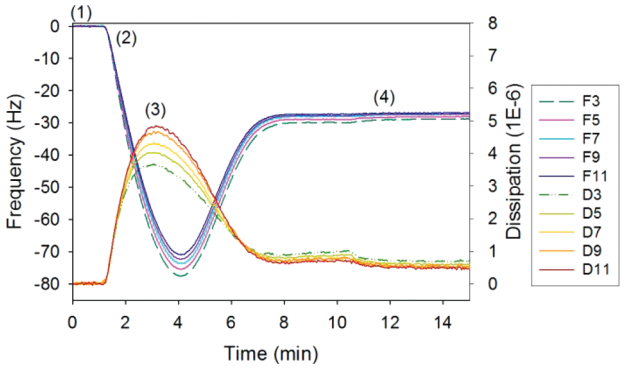

Figure 3. Typical QCM-D response for PC bilayer formation. (1) Initial buffer baseline, (2) vesicle deposition, (3) vesicle rupture and release of water, (4) stable bilayer. The lines represent different overtone responses for frequency and dissipation.

stabilized. Each experiment was repeated at least three times for each concentration of chrysophsin-3.

RESULTS

Bilayer formation was monitored by observing patterns in QCM-D frequency and dissipation responses. During bilayer formation, lipid vesicles first attach to the QCM-D sensor surface, adding mass. The vesicles then burst, releasing the fluid within the vesicle and creating a supported lipid bilayer.[31,32] Typically, the frequency decreased by ~80 Hz when vesicles adsorbed and showed an increase as soon as the vesicles ruptured to form the bilayer (Figure 3). The dissipation showed a characteristic increase to $\sim 6 \times 10^{-6}$ in response to the attachment of the water-filled vesicles. After bilayer formation, dissipation decreased because the bilayer is more rigid than vesicles. A complete bilayer could be characterized by a final Δf of ~26 Hz and change in dissipation (ΔD) of $\sim 1 \times 10^{-6}$ in the third harmonic.

When peptide was added and allowed to remain in contact with the bilayer, changes in frequency and dissipation were monitored continuously for ~60 min (Figure 4). Typical frequency responses at all overtones showed an initial decrease in frequency, and therefore an increase in mass, on the crystal as peptides attached to the bilayer (Figure 5). The frequency response produced using the 0.05 μM solution of chrysophsin-3 showed the smallest change of the concentrations tested (Figure 5A). Between chrysophsin-3 concentrations of 0.25 and 2 μM, the frequency decreased up to several Hertz upon peptide exposure (Figure 5B–D). At higher chrysophsin-3 concentrations, dissipation values increased upon the sensor's contact with the peptide solution, suggesting that the film upon the sensor crystal became less rigid or more saturated with fluid (Figure 4B). The subsequent buffer rinse resulted in a decrease in mass on the crystal and a more rigid film. Exposure to peptide at 4 and 10 μM concentrations also caused Δf to decrease rapidly, and this gradually stabilized to a value between −6 and −7 Hz, suggesting that the peptides approached a critical concentration on the supported lipid bilayer surface (Figure 5E–F).

Data were analyzed in terms of Δf and ΔD at all measured overtones before and after the final buffer rinse. The first measurement represents the stable state reached after 1 h of peptide exposure, while the second measurement taken after the buffer rinse shows the irreversible change due to peptide–bilayer interactions. The Δf was calculated by taking the difference between

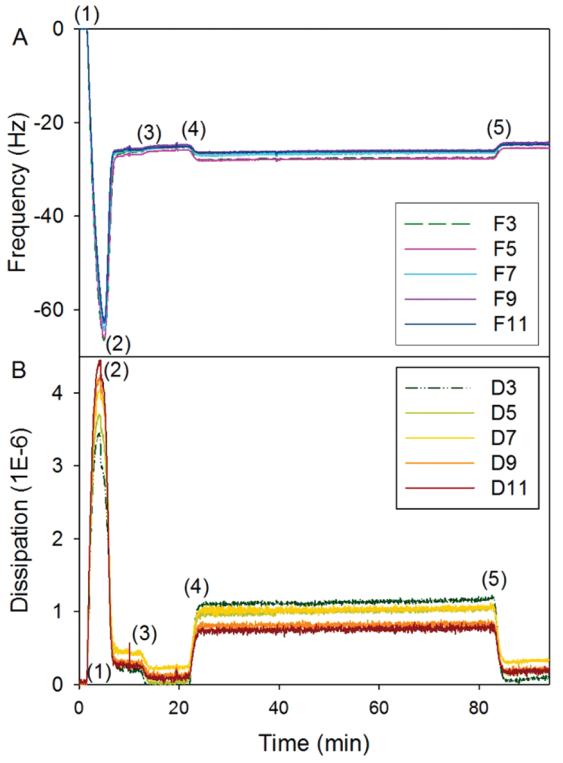

Figure 4. Typical frequency (A) and dissipation (B) responses for PC bilayer formation and subsequent chrysophsin-3 deposition. This experiment represents a chrysophsin-3 concentration of 4 μM. (1) Initial buffer baseline, (2) lipid vesicle deposition, (3 and 5) buffer rinse, (4) peptide addition.

frequencies at the beginning of peptide exposure and before (Figures 6 and 7) or after the subsequent buffer rinse (Figures 8 and 9)[23]

$$\Delta f = (\Delta f_{\text{bilayer and peptide}} - \Delta f_{\text{bilayer}})\frac{1}{n} \quad (4)$$

At a very low concentration (0.05 μM chrysophsin-3), the peptide did not destabilize the bilayer, and Δf and ΔD were typically small, positive, and uniform across all overtones (Figures 6A, 7A, 8A, 9A). The average Δf for 0.25 μM chrysophsin-3 was between −0.7 and −1.0 Hz (Figures 6B and 8B), and the average ΔD was positive (Figures 7B and 9B). At intermediate chrysophsin-3 concentrations of 1, 2, and 4 μM, the greatest decreases in frequency and increases in dissipation occurred at the third harmonic. The changes became less pronounced at higher overtones (Figures 6C–E, 7C–E, 8C–E, and 9C–E). For the highest concentration tested (10 μM chrysophsin-3), nonhomogeneous Δf and ΔD values were produced at the stable stage before the buffer rinse (Figures 6F and 7F). However, positive Δf values were observed at all overtones after the buffer rinse (Figure 8F), while the ΔD values were lower than those for 1, 2, and 4 μM and before the buffer rinse (Figure 9 F).

DISCUSSION

Formation of Supported Lipid Bilayer. The Δf values corresponding to PC bilayer formation were compared to published values.[20] According to prior researchers, a PC bilayer on silica corresponds to an initial Δf of about −70 Hz and a net change of

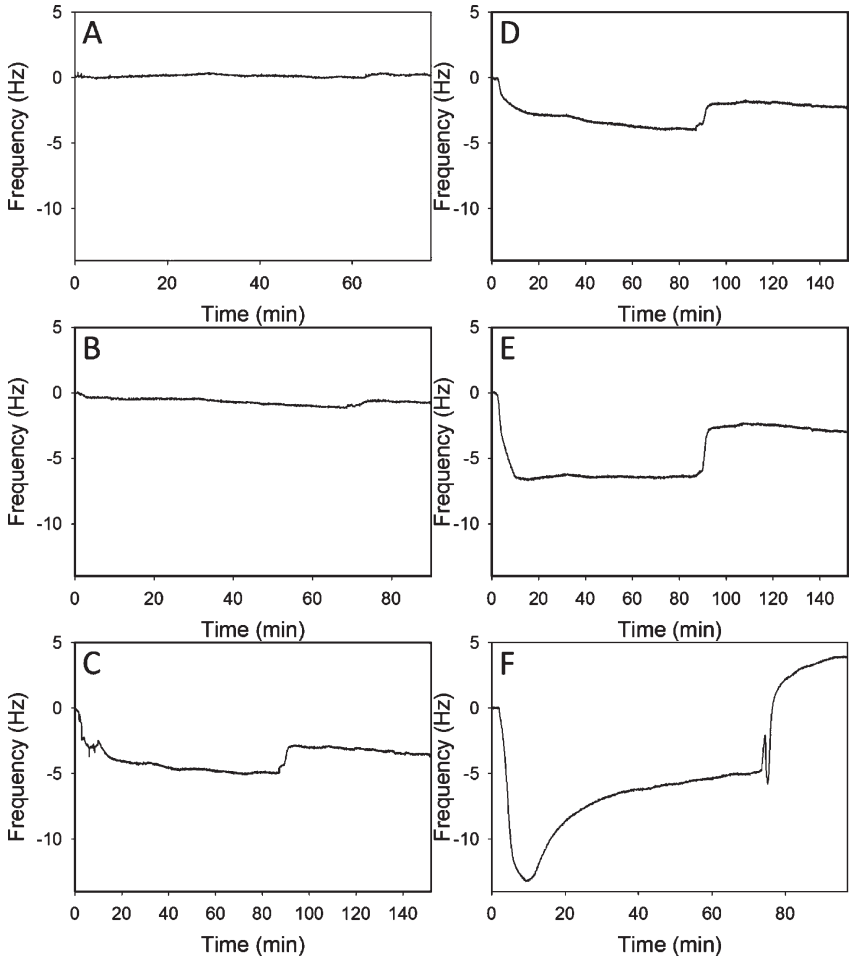

Figure 5. Typical QCM-D responses in the third harmonic for PC bilayers exposed to chrysophsin-3 at (A) 0.05 μM, (B) 0.25 μM, (C) 1 μM, (D) 2 μM, (E) 4 μM, and (F) 10 μM chrysophsin-3 concentrations. The initial time of 0 min corresponds to time position (4) in Figure 4, and the final buffer rinse occurs at about 70−80 min, which corresponds to time position (5) in Figure 4.

−26 Hz, which are similar to what we observed. However, our initial Δf was slightly higher at −80 Hz, which may be attributed to the use of Texas Red DHPE in this previous study, which we did not use.[20] Supported PC bilayers can be made reproducibly and easily on silica surfaces, which has led to them being used widely as model cell membranes.[24,32,33]

Mechanism of Chrysophsin-3 Action on PC Bilayer. Once formation of the PC bilayer was validated through Δf and ΔD data, various concentrations of chrysophsin-3 were introduced to the membrane. At 0.05 μM chrysophsin-3, small Δf values (<1 Hz) were observed for each overtone (Figures 6A and 8A) and small, positive ΔD values were recorded before and after the final buffer rinse (Figures 7A and 9A). These results indicate that little or no mass change occurred in the bilayer. A small Δf (∼0.4−0.7 Hz) was seen in the third harmonic, which indicates a small amount of nonhomogeneity in AMP action. The difference was not uniform at all overtones and the positive Δf indicates that small amounts of mass are being removed after the final buffer rinse. Only a small fraction of lipid mass was removed, however, since the Δf values were much less than 26 Hz, which corresponds to removal of the full bilayer.

The frequency data for 0.25 μM chrysophsin-3 resulted in Δf values of ∼−1 Hz (Figures 6B and 8B) and positive ΔD for all recorded overtones before and after the buffer rinse (Figures 7B and 9B), which indicates that the final buffer rinse did not significantly affect the mass and viscoelasticity of the membrane. Relatively uniform mass changes were observed at all measured overtones of the bilayer, which indicates that mass changes were homogeneous at all depths of the bilayer. The positive ΔD values observed at all overtones suggest that the membrane became less rigid with the addition of peptide. The Δf and ΔD data combined indicate cylindrical pore formation may have occurred, as peptides are positioned perpendicularly through the lipid bilayer and the mass changes at all depths are similar (Figure 10A). Also, the creation of pores would allow more water to enter the membrane space, making the film less rigid. At the third harmonic, a mass change similar to that of the other overtones was observed. Therefore, the peptides that attached to the SLB likely formed pores and did not remain on the bilayer surface, which would have resulted in heterogeneous changes and nonuniform responses. The difference in results at these low concentrations indicates that chrysophsin-3 will begin to form pores in the PC membrane at some critical concentration between 0.05 and 0.25 μM.

At 1, 2, and 4 μM concentrations, the third harmonic exhibited the most mass addition (Δf) after peptide exposure and after the final buffer rinse. The other Δf values decreased in absolute magnitude with increasing overtones (Figures 6C−E and

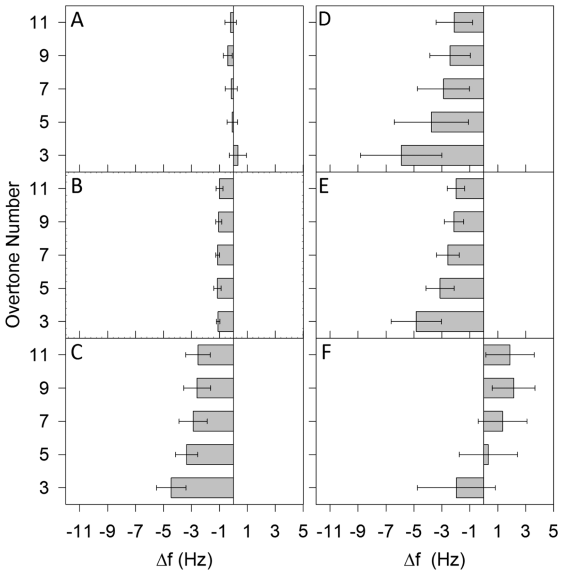

Figure 6. Average Δf at different overtones for (A) 0.05 μM, (B) 0.25 μM, (C) 1 μM, (D) 2 μM, (E) 4 μM, and (F) 10 μM chrysophsin-3 concentrations, before the buffer rinse. The graphs show the amount of mass that is attached to or removed from the bilayer after the SLB was exposed to chrysophsin-3 for 1 h.

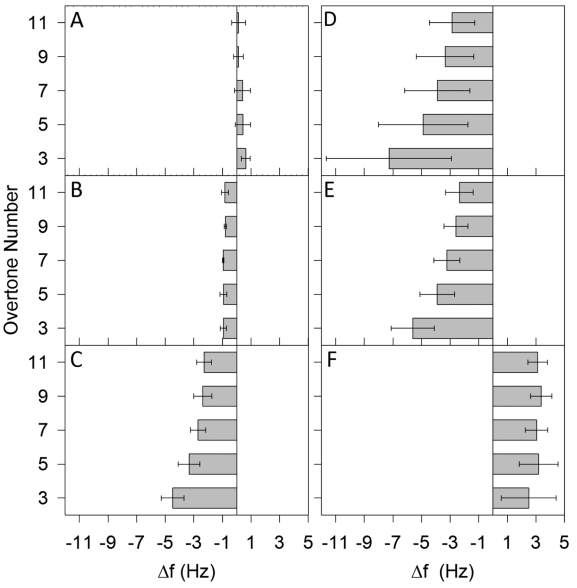

Figure 8. Average Δf at different overtones for (A) 0.05 μM, (B) 0.25 μM, (C) 1 μM, (D) 2 μM, (E) 4 μM, and (F) 10 μM chrysophsin-3 concentrations, after the buffer rinse. The changes show the amount of mass that is not removed by the final buffer rinse and is irreversibly attached to the crystal surface.

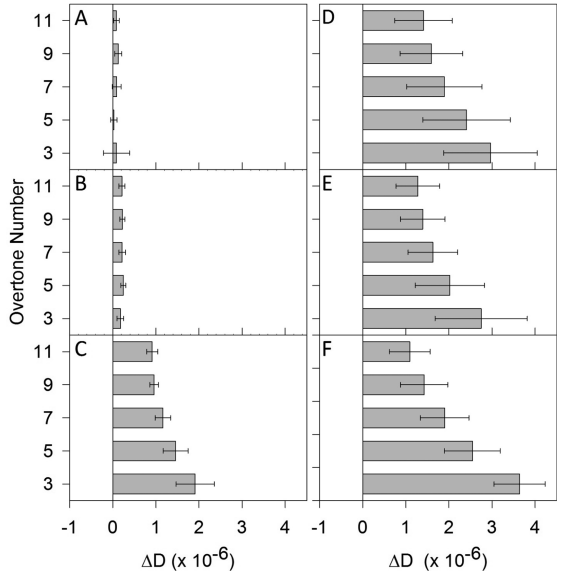

Figure 7. Average ΔD at different overtones for (A) 0.05 μM, (B) 0.25 μM, (C) 1 μM, (D) 2 μM, (E) 4 μM, and (F) 10 μM chrysophsin-3 concentrations, before the buffer rinse. The changes reveal the homogeneous (at 0.05 and 0.25 μM concentrations) and heterogeneous (at larger concentrations) nature of the viscosity of the mass after exposure of the lipid bilayer to chrysophsin-3 for 1 h.

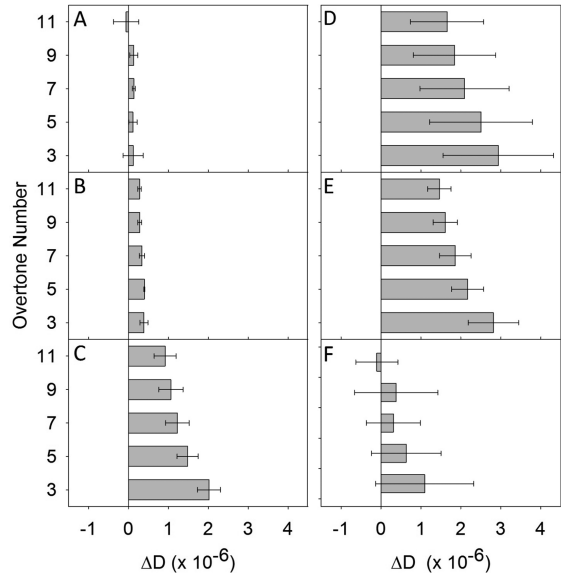

Figure 9. Average ΔD at different overtones for (A) 0.05 μM, (B) 0.25 μM, (C) 1 μM, (D) 2 μM, (E) 4 μM, and (F) 10 μM chrysophsin-3 concentrations, after the buffer rinse.

8C−E). The third harmonic also demonstrated behavior of a less rigid film (ΔD) compared to the other harmonics, which also decreased as the overtones increased (Figures 7C−E and 9C−E). This indicates that the mass changes and viscoelasticity changes were heterogeneous throughout the membrane. One possible interpretation of these results is a large amount of peptide absorbed to the bilayer surface, resulting in nonuniform change in the bilayer. The ΔD results suggest that the film may be "softer" at the liquid−membrane interface due to the presence of water between the peptide molecules and the less rigid structure of the peptides adsorbed to the membranes. Since chrysophsin-3 formed cylindrical pores at 0.25 μM, the system likely consists of both pores and adsorbed AMPs at 1, 2, and 4 μM concentrations. In the proposed mechanism, the peptides adsorbed onto the surface of the SLB and formed pores in the membrane, as in the barrel-stave model (Figure 10B, C). The frequency response curve for 4 μM chrysophsin-3 shows the AMPs adsorbed on the lipid membrane rapidly reaching saturation, due to the Δf reaching steady state at −6.5 Hz (Figure 5E).

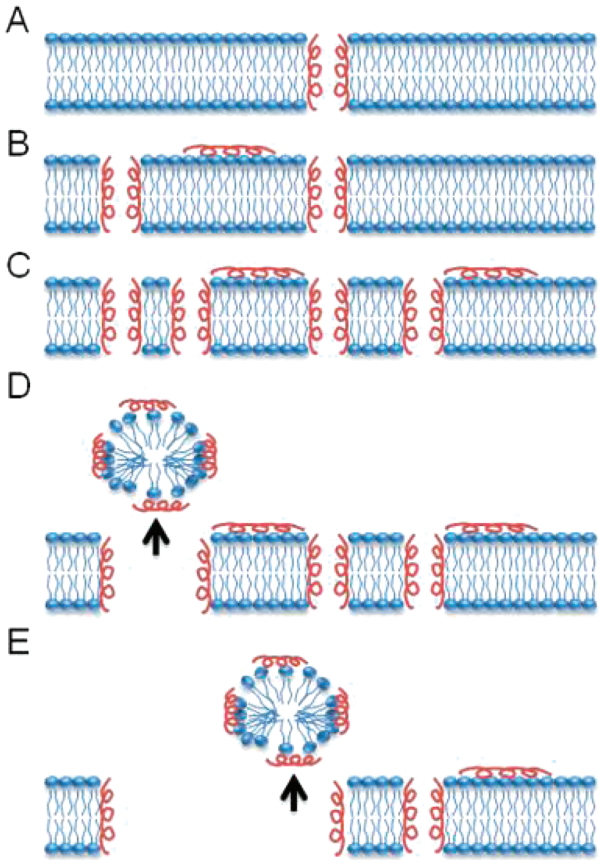

Figure 10. Proposed mechanism of chrysophsin-3 action on a supported PC bilayer as a function of peptide concentration. (A) At low chrysophsin-3 concentrations (~0.25 μM), peptides prefer insertion into the membrane over adsorption onto the surface. (B) As the concentration increases (~1 μM), peptides continue to form pores and begin to adsorb onto the bilayer surface. (C) The amount of peptides adsorbed on the bilayer surface and inserted to form pores increases (~2 μM). (D) At a certain critical concentration (~4 μM), peptide–lipid aggregates begin to be removed from the membrane. (E) Large concentrations of chrysophsin-3 (~10 μM) result in the loss of large areas of the bilayer.

At a concentration of 10 μM, chrysophsin-3 addition to the PC bilayer resulted in negative Δf values at the third harmonic and positive Δf values at higher overtones after 1 h of peptide exposure (Figure 6F). However, the buffer rinse produced uniform positive Δf values at all overtones (Figure 8F). The raw frequency data showed an initial mass addition on the PC bilayer surface upon exposure to the AMP, followed by a decrease in mass that seemed to approach steady state (Figure 5F). These results suggest that at high concentrations chrysophsin-3 initially adsorbs to the surface of the bilayer, forms pores in the membrane, and gradually causes mass removal, which may be in the form of peptide–lipid aggregates (Figure 10D, E). The mass loss was also increased by rinsing the system with buffer. The dissipation results suggest that the film became less rigid after 1 h of peptide exposure (Figure 7F) but more rigid after the buffer rinse (Figure 9F). The membrane also became more rigid with 10 μM chrysophsin-3 than it did at lower chrysophsin-3 concentrations. This could be due to the remaining large "islands", or areas, of lipids on the crystal surface surrounded by large regions of water created by mass lipid removal. The water may not be incorporated into the membrane as it is when there are fewer pores in the membrane, causing the measured film to be composed of the more rigid PC bilayer.

Mechler et al. followed a similar procedure to investigate the action of the peptides caerin 1.1, maculatin 1.1, and aurein 1.2 on DMPC and DMPC/DMPG (4:1) bilayers using QCM-D. The negative Δf resulting from chrysophsin-3 in this experiment correlated most closely with those of caerin 1.1, a 25-amino acid AMP isolated from the skin of the Australian tree frog.[23] Like chrysophsin-3, caerin 1.1 also exhibits an amphipathic α-helical conformation at the cell membrane surface.[34] On a DMPC bilayer, larger Δf values were measured for the 10 and 20 μM caerin 1.1 concentrations, which were significantly larger than those used in this study. The results for maculatin 1.1 revealed a critical concentration between 5 and 7 μM at which the system transitioned between overall mass removal and mass addition. Aurein 1.2 also appeared to exhibit different behavior at higher overtones between 7 and 10 μM solutions. The much smaller critical concentration of chrysophsin-3 may be attributed to the difference in peptide composition and structure, as well as to the different lipids used in the membrane. Chrysophsin-3 has a higher molecular weight than aurein 1.2 and maculatin 1.1.[16,23] Also, DMPC has a lower molecular weight than PC, the latter of which may be more conducive to pore formation.

Relating QCM-D Results to Chrysophsin-3 Activity Against Bacteria. Pore formation can represent the start of the killing process in bacteria. Chrysophsin-3 has been tested for its antimicrobial activity against some Gram-negative and Gram-positive bacteria, although the lethal concentration is different for each case. Iijima et al. found 0.25 μM to be the minimal lethal concentration of chrysophsin-3 required to kill 99% of *Bacillus subtilis* or *Escherichia coli*. Certain strains of Gram-positive and Gram-negative pathogenic bacteria, such as *Lactococcus garvieae* and *Vibrio anguillarum*, required 10 μM synthetic chrysophsin-3 to achieve the same level of killing, while other strains were resistant or required as low as 5 μM chrysophsin-3.[16] Research from our laboratory has shown that 0.22 mM chrysophsin-3, with added inosine and L-alanine, was needed to kill 99% of spores of *B. anthracis*, the cause of anthrax, and this killing occurred within one hour of exposure. Inosine and L-alanine are germination agents that promote the breakdown of the spore coat. Without any germinants, the same concentration of chrysophsin-3 killed about 80% of *B. anthracis* spores.[35]

In QCM-D experiments, we showed that at 0.25 μM chrysophsin-3 pore formation began to develop along the thickness of the membrane. At a much higher concentration of 10 μM, pore formation was greater, and more mass was lost from the lipid bilayer membrane. These results seem consistent with the observed range of experimental lethal concentrations on bacterial cells. It is not yet known how specific differences in the lipid composition affect the ability to break down the membrane. The lipid PC, which we used in the present studies, has a zwitterionic headgroup. This is similar to the zwitterionic headgroup of *E. coli* and other Gram-negative bacterial membrane lipids.[36] Gram-positive bacteria, including *Bacillus spp.*, have negatively charged headgroups in their lipid membranes.[36]

CONCLUSIONS

QCM-D frequency and dissipation data were used to elucidate the mechanism of AMP action on SLBs. Our results demonstrate that the nature of chrysophsin-3 interactions with a PC bilayer is

concentration-dependent. The AMP appears to destabilize the model membrane by forming pores and leaving the bilayer via peptide−lipid aggregates. QCM-D was shown to be an effective technique for studying AMP and SLB interactions. This method can be applied to other systems of peptides and lipid bilayers to provide a better understanding of AMP action on cell membranes.

AUTHOR INFORMATION

Corresponding Author

*Phone: 508.831.5380. Fax: 508.831.5853. E-mail: terric@wpi.edu.

ACKNOWLEDGMENT

We would like to thank Dr. Matthew C. Dixon (Biolin Scientific Inc.) for helpful discussions about QCM-D analysis. We thank Professor Alain Brisson (IECB) and Dr. Nam-Joon Cho (Stanford University) for useful discussions regarding preparing supported lipid bilayers. This work was supported by funding from the Natick Soldier Research, Development & Engineering Center (NSRDEC).

REFERENCES

(1) Skarnes, R. C.; Watson, D. W. *Bacteriol. Rev.* **1957**, *21*, 273–294.
(2) Gazit, E.; Miller, I. R.; Biggin, P. C.; Sansom, M. S.; Shai, Y. *J. Mol. Biol.* **1996**, *258*, 860–870.
(3) Fulmer, P. A.; Lundin, J. G.; Wynne, J. H. *ACS Appl. Mater. Interfaces* **2010**, *2*, 1266–1270.
(4) Decraene, V.; Pratten, J.; Wilson, M. *Appl. Environ. Microbiol.* **2006**, *72*, 4436–4439.
(5) Fritsche, T. R.; Rhomberg, P. R.; Sader, H. S.; Jones, R. N. *J. Antimicrob. Chemother.* **2008**, *61*, 1092–1098.
(6) Steiner, H.; Andreu, D.; Merrifield, R. B. *Biochim. Biophys. Acta* **1988**, *939*, 260–266.
(7) Gregory, K.; Mello, C. M. *Appl. Environ. Microbiol.* **2005**, *71*, 1130–1134.
(8) Boman, H. G.; Agerberth, B.; Boman, A. *Infect. Immun.* **1993**, *61*, 2978–2984.
(9) Brogden, K. A. *Nat. Rev. Microbiol.* **2005**, *3*, 238–250.
(10) Shai, Y. *Biopolymers* **2002**, *66*, 236–248.
(11) Pouny, Y.; Rapaport, D.; Mor, A.; Nicolas, P.; Shai, Y. *Biochemistry* **1992**, *31*, 12416–12423.
(12) Shai, Y.; Oren, Z. *Peptides* **2001**, *22*, 1629–1641.
(13) Shai, Y. *Biochim. Biophys. Acta* **1999**, *1462*, 55–70.
(14) Huang, H. W. *Biochemistry* **2000**, *39*, 8347–8352.
(15) Cole, A. M.; Darouiche, R. O.; Legarda, D.; Connell, N.; Diamond, G. *Antimicrob. Agents Chemother.* **2000**, *44*, 2039–2045.
(16) Iijima, N.; Tanimoto, N.; Emoto, Y.; Morita, Y.; Uematsu, K.; Murakami, T.; Nakai, T. *Eur. J. Biochem.* **2003**, *270*, 675–686.
(17) Zhang, L.; Parente, J.; Harris, S. M.; Woods, D. E.; Hancock, R. E.; Falla, T. J. *Antimicrob. Agents Chemother.* **2005**, *49*, 2921–2927.
(18) Mason, A. J.; Bertani, P.; Moulay, G.; Marquette, A.; Perrone, B.; Drake, A. F.; Kichler, A.; Bechinger, B. *Biochemistry* **2007**, *46*, 15175–15187.
(19) Tamm, L. K.; McConnell, H. M. *Biophys. J.* **1985**, *47*, 105–113.
(20) Keller, C. A.; Kasemo, B. *Biophys. J.* **1998**, *75*, 1397–1402.
(21) Thid, D.; Benkoski, J. J.; Svedhem, S.; Kasemo, B.; Gold, J. *Langmuir* **2007**, *23*, 5878–5881.
(22) Wittmer, C. R.; Phelps, J. A.; Saltzman, W. M.; Van Tassel, P. R. *Biomaterials* **2007**, *28*, 851–860.
(23) Mechler, A.; Praporski, S.; Atmuri, K.; Boland, M.; Separovic, F.; Martin, L. L. *Biophys. J.* **2007**, *93*, 3907–3916.
(24) Cremer, P. S. a. B.; Steven, G. *J. Phys. Chem.* **1999**, *103*, 2554–2559.
(25) Salafsky, J.; Groves, J. T.; Boxer, S. G. *Biochemistry* **1996**, *35*, 14773–14781.
(26) Barenholz, Y.; Gibbes, D.; Litman, B. J.; Goll, J.; Thompson, T. E.; Carlson, R. D. *Biochemistry* **1977**, *16*, 2806–2810.
(27) Kanazawa, K. K.; Gordon, J. G., II *Anal. Chim. Acta* **1985**, *175*, 99–105.
(28) Voinova, M. V.; Jonson, M.; Kasemo, B. *Biosens. Bioelectron.* **2002**, *17*, 835–841.
(29) Voinova, M. V.; Rodahl, M.; Jonson, M.; Kasemo, B. *Phys. Scr.* **1999**, *59*, 391–396.
(30) Bordes, R.; Höök, F. *Anal. Chem.* **2010**, *82*, 9116–9121.
(31) Richter, R.; Mukhopadhyay, A.; Brisson, A. *Biophys. J.* **2003**, *85*, 3035–3047.
(32) Keller, C. A.; Glasmastar, K.; Zhdanov, V. P.; Kasemo, B. *Phys. Rev. Lett.* **2000**, *84*, 5443–5446.
(33) Schonherr, H.; Johnson, J. M.; Lenz, P.; Frank, C. W.; Boxer, S. G. *Langmuir* **2004**, *20*, 11600–11606.
(34) Stone, D. J. M.; Waugh, R. J.; Bowie, J. H.; Wallace, J. C.; Tyler, J. C. *J. Chem. Soc., Perkin Trans.* **1992**, *1*, 3173–3178.
(35) Pinzón-Arango, P. A.; Nagarajan, R.; Camesano, T. A., submitted.
(36) Blondelle, S. E.; Lohner, K.; Aguilar, M. *Biochim. Biophys. Acta* **1999**, *1462*, 89–108.